

Representations for the Marchenko method for imperfectly sampled data

Kees Wapenaar and Johno van IJsseldijk, Delft University of Technology

Summary

The Marchenko method is based on two integral representations for focusing functions and Green's functions. In practice the integrals are replaced by finite summations. This works well for regularly sampled data, but the quality of the results degrade in case of imperfect sampling. We reformulate the integral representations into summation representations which properly account for imperfectly sampled data and we illustrate these representations with numerical examples. We indicate how these representations may be used to modify the Marchenko method to account for imperfect sampling.

Introduction

The Marchenko method has been introduced as a data-driven approach to deal with internal multiples in seismic imaging (Broggini and Snieder, 2012; Wapenaar et al., 2014b; Ravasi et al., 2016; Staring et al., 2018; Pereira et al., 2018) and for monitoring and forecasting the wave field of induced seismic sources (Van der Neut et al., 2017; Brackenhoff et al., 2019). Central in the Marchenko method are two integral representations, which formulate mutual relations between the reflection response at the surface, focusing functions and Green's functions with virtual sources and/or receivers in the subsurface. Given the reflection data at the surface and an initial estimate of the focusing functions, these integral representations can be solved for the focusing functions and Green's functions, which can subsequently be used for imaging and monitoring.

The aforementioned representations consist of integrals along sources and/or receivers at the surface from minus infinity to plus infinity. In practice these representations are discretized and truncated prior to solving them. This works well for regularly sampled data on a large enough grid and obeying the Nyquist criterion. Most authors that use the Marchenko method tacitly assume that these conditions are fulfilled. Staring and Wapenaar (2019) numerically evaluate the effects of missing near offsets, limited crossline aperture and undersampling in the crossline direction on the 3D Marchenko method.

The aim of this paper is to reformulate the integral representations underlying the Marchenko method in terms of discrete finite summations, such that they account for imperfectly sampled data. This problem is akin to reformulating the representations underlying seismic interferometry for irregular source distributions. For seismic interferometry the approach is as follows. The classical correlation integral representation (Wapenaar and Fokkema, 2006) is replaced by a convolution integral representation, which is subsequently inverted by multidimensional deconvolution (Wapenaar and van der Neut, 2010). The point-spread function plays a central role in this approach (Van der Neut and Wapenaar, 2015). Here we introduce a variant of this approach, leading to summation representations for the Marchenko method, including point-spread functions. We illustrate these representations with numerical examples. This is the first step towards modifying the Marchenko method for

imperfectly sampled data. The second step, resolving the summation representations, is subject of ongoing research.

Integral representations

We start with flux-normalised acoustic representations, which read in the space-time (\mathbf{x}, t) domain (Wapenaar et al., 2014a)

$$G^{-,+}(\mathbf{x}_R, \mathbf{x}_A, t) + f_1^-(\mathbf{x}_R, \mathbf{x}_A, t) = \quad (1)$$

$$\int_{\partial\mathbb{D}_0} R(\mathbf{x}_R, \mathbf{x}, t) * f_1^+(\mathbf{x}, \mathbf{x}_A, t) d\mathbf{x},$$

$$G^{-,-}(\mathbf{x}_R, \mathbf{x}_A, t) + f_1^+(\mathbf{x}_R, \mathbf{x}_A, -t) = \quad (2)$$

$$\int_{\partial\mathbb{D}_0} R(\mathbf{x}_R, \mathbf{x}, t) * f_1^-(\mathbf{x}, \mathbf{x}_A, -t) d\mathbf{x}.$$

The asterisks (*) denote temporal convolution. $\partial\mathbb{D}_0$ denotes the acquisition surface, which is considered to be reflection free (this corresponds to the situation after surface-related multiple elimination). $R(\mathbf{x}_R, \mathbf{x}, t)$ is the reflection response of the inhomogeneous medium below $\partial\mathbb{D}_0$, with \mathbf{x} and \mathbf{x}_R at $\partial\mathbb{D}_0$. The focusing functions $f_1^+(\mathbf{x}, \mathbf{x}_A, t)$ and $f_1^-(\mathbf{x}, \mathbf{x}_A, t)$ are defined in a truncated medium, which is identical to the actual medium between $\partial\mathbb{D}_0$ and $\partial\mathbb{D}_A$ and reflection free below $\partial\mathbb{D}_A$. Here $\partial\mathbb{D}_A$ is a horizontal surface below $\partial\mathbb{D}_0$. It is chosen such that it contains the focal point \mathbf{x}_A of the focusing function. The focusing function $f_1^+(\mathbf{x}, \mathbf{x}_A, t)$ is shaped such that, when emitted from $\partial\mathbb{D}_0$ into the truncated medium, it focuses at \mathbf{x}_A . The function $f_1^-(\mathbf{x}, \mathbf{x}_A, t)$ is the reflection response of the truncated medium to $f_1^+(\mathbf{x}, \mathbf{x}_A, t)$. $G^{-,+}(\mathbf{x}_R, \mathbf{x}_A, t)$ and $G^{-,-}(\mathbf{x}_R, \mathbf{x}_A, t)$ are the upgoing parts of the Green's functions at \mathbf{x}_R , in response to sources for downgoing (+) and upgoing (-) waves, respectively, at \mathbf{x}_A . These Green's functions are defined in the actual medium. For further details we refer to the aforementioned papers about the Marchenko method.

We illustrate equations (1) and (2) with a 2D numerical example. We consider a horizontally layered medium, with $\partial\mathbb{D}_0$ at $x_3 = 0$ m, three interfaces at 450, 850 and 1100 m, propagation velocities of 1000, 2000, 2250 and 3000 m/s, and mass densities with the same numerical values as the velocities (but in kg/m^3). The focal point is defined as $\mathbf{x}_A = (0, 1000)$ m. We numerically model the reflection response at $\partial\mathbb{D}_0$ and convolve it with a Ricker wavelet with a central frequency of 25 Hz. Also the focusing functions are numerically modeled (since in this paper we want to evaluate representations instead of the performance of the Marchenko method). We evaluate the integrals in the right-hand sides of equations (1) and (2), using regular sampling ($\Delta x = 5$ m, nr. of samples is 1001). The results are shown in Figures 1(a) and (b), respectively.

In practice, the right-hand sides of equations (1) and (2) are approximated by

$$\sum_i R(\mathbf{x}_R, \mathbf{x}^{(i)}, t) * f_1^+(\mathbf{x}^{(i)}, \mathbf{x}_A, t) * S(t), \quad (3)$$

$$\sum_i R(\mathbf{x}_R, \mathbf{x}^{(i)}, t) * f_1^-(\mathbf{x}^{(i)}, \mathbf{x}_A, -t) * S(t), \quad (4)$$

Marchenko representations for imperfectly sampled data

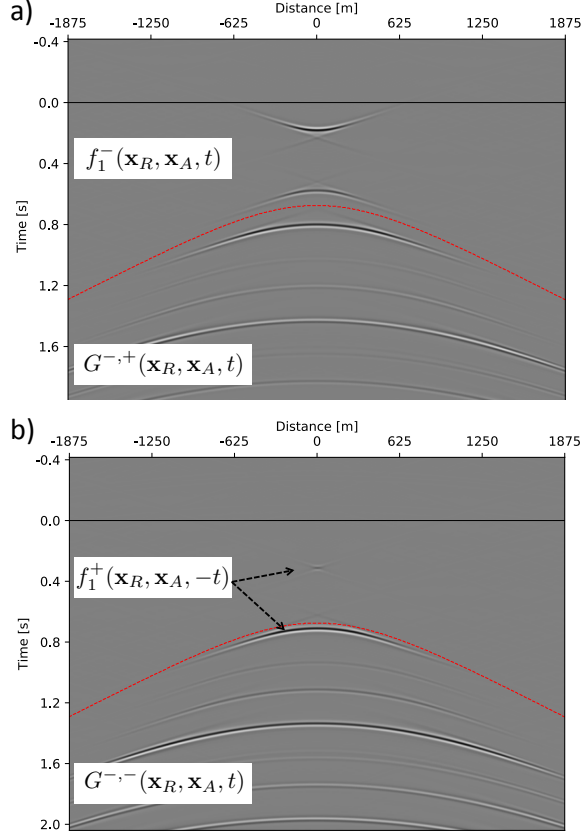


Figure 1: Evaluation of the integrals in equations (1) and (2), for fixed \mathbf{x}_A at $\partial\mathbb{D}_A$ and variable \mathbf{x}_R along $\partial\mathbb{D}_0$. The red dashed lines separate the recovered focusing functions from the Green's functions at the left-hand sides of these equations (except for the first event below the red line in (b), which belongs to the focusing function and the Green's function).

with $\mathbf{x}^{(i)}$ at $\partial\mathbb{D}_0$ and $S(t)$ the source wavelet. Assuming $\mathbf{x}^{(i)}$ is imperfectly sampled (irregular sampling, spatial aliasing, missing small offsets, finite aperture, etc.), these approximations have an effect on the recovered focusing functions and Green's functions. We illustrate this with a numerical example, for the situation of irregular source sampling. Figure 2 shows an irregular distribution of sample points $\mathbf{x}^{(i)}$ along $\partial\mathbb{D}_0$ (average $\Delta x = 10$ m, nr. of samples is 501). We evaluate equations (3) and (4), using the same numerically modeled reflection response and focusing functions as in the previous example. The results are shown in Figures 3(a) and (b), respectively. Comparing this with Figure 1 reveals the effects of the imperfect sampling. In the following we quantify this effect.



Figure 2: Irregular distribution of $\mathbf{x}^{(i)}$ along $\partial\mathbb{D}_0$. The black bars denote the positions of the samples.

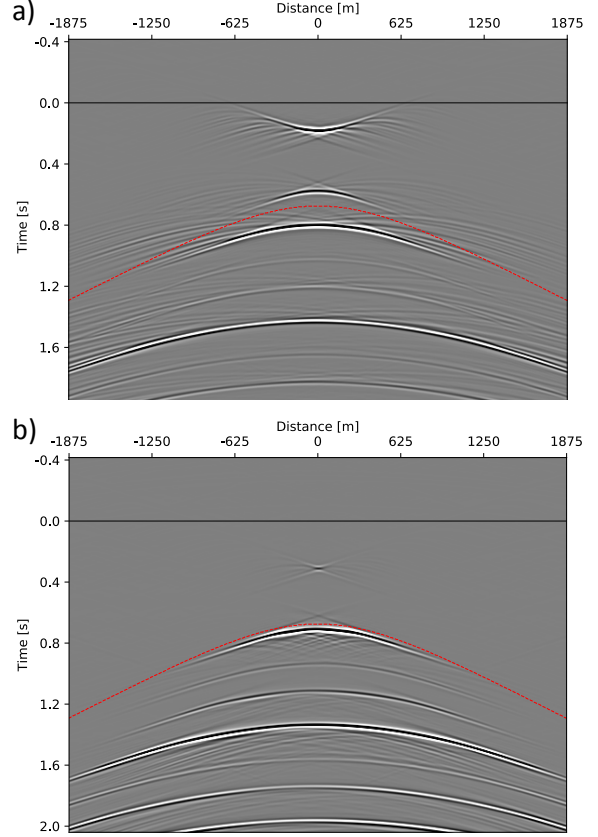


Figure 3: Evaluation of the irregular summations in equations (3) and (4), for fixed \mathbf{x}_A at $\partial\mathbb{D}_A$ and variable \mathbf{x}_R along $\partial\mathbb{D}_0$.

Point-spread functions

We discuss some properties of the focusing functions and introduce point-spread functions. These will be used in the next section to transform the integral representations of equations (1) and (2) into summation representations.

The focusing function f_1^+ is defined as the inverse of the transmission response T between $\partial\mathbb{D}_0$ and $\partial\mathbb{D}_A$ (Wapenaar et al., 2014a). This is quantified as follows

$$\delta(\mathbf{x}'_{H,A} - \mathbf{x}_{H,A})\delta(t) = \int_{\partial\mathbb{D}_0} T(\mathbf{x}'_A, \mathbf{x}, t) * f_1^+(\mathbf{x}, \mathbf{x}_A, t) d\mathbf{x}, \quad (5)$$

with \mathbf{x}'_A and \mathbf{x}_A at $\partial\mathbb{D}_A$, and $\mathbf{x}'_{H,A}$ and $\mathbf{x}_{H,A}$ denoting the horizontal coordinates of \mathbf{x}'_A and \mathbf{x}_A , respectively. An alternative way to quantify this relation is

$$\delta(\mathbf{x}_H - \mathbf{x}'_H)\delta(t) = \int_{\partial\mathbb{D}_A} f_1^+(\mathbf{x}, \mathbf{x}_A, t) * T(\mathbf{x}_A, \mathbf{x}', t) d\mathbf{x}_A, \quad (6)$$

with \mathbf{x} and \mathbf{x}' at $\partial\mathbb{D}_0$. To keep the focusing function stable, evanescent waves are excluded. This implies that the integral in equation (5) or (6) yields a band-limited approximation of the delta function in the left-hand side. This is illustrated in Figure 4, which is obtained by evaluating the integral in equation (5) numerically, using regular sampling ($\Delta x = 5$ m, nr. of samples is 1001). Note that the sifting property of the

Marchenko representations for imperfectly sampled data

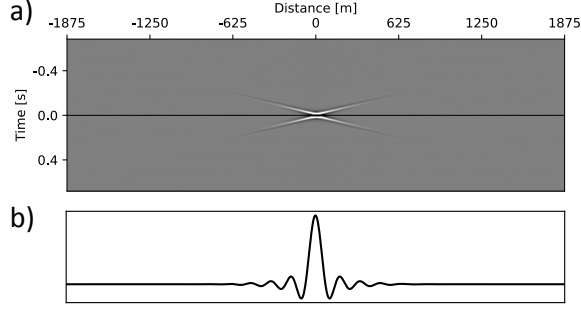


Figure 4: (a) Evaluation of the integral in equation (5). (b) Cross-section of the Fourier transform of (a) for the central frequency component (25 Hz). This is a spatially band-limited delta function. The width of the main lobe is 150 m.

delta function, $h(\mathbf{x}_H) = \int \delta(\mathbf{x}_H - \mathbf{x}'_H) h(\mathbf{x}'_H) d\mathbf{x}'_H$, is also valid for a spatially band-limited delta function, assuming $h(\mathbf{x}_H)$ is also spatially band-limited (which is the case when evanescent waves are excluded). We use this property in the next section. In a similar way we define a quantity Y as the inverse of the time-reversal of f_1^- , as follows

$$\delta(\mathbf{x}'_{H,A} - \mathbf{x}_{H,A}) \delta(t) = \int_{\partial \mathbb{D}_0} Y(\mathbf{x}'_A, \mathbf{x}, t) * f_1^-(\mathbf{x}, \mathbf{x}_A, -t) d\mathbf{x}, \quad (7)$$

or

$$\delta(\mathbf{x}_H - \mathbf{x}'_H) \delta(t) = \int_{\partial \mathbb{D}_A} f_1^-(\mathbf{x}, \mathbf{x}_A, -t) * Y(\mathbf{x}_A, \mathbf{x}', t) d\mathbf{x}_A. \quad (8)$$

Note that this inverse may be unstable (since $f_1^-(\mathbf{x}, \mathbf{x}_A, t)$ is a reflection response), so it should be handled with care.

For the case of imperfect sampling, the discretised band-limited versions of equations (5) and (7) read

$$\Gamma^+(\mathbf{x}'_A, \mathbf{x}_A, t) = \sum_i T(\mathbf{x}'_A, \mathbf{x}^{(i)}, t) * f_1^+(\mathbf{x}^{(i)}, \mathbf{x}_A, t) * S(t) \quad (9)$$

and

$$\Gamma^-(\mathbf{x}'_A, \mathbf{x}_A, t) = \sum_i Y(\mathbf{x}'_A, \mathbf{x}^{(i)}, t) * f_1^-(\mathbf{x}^{(i)}, \mathbf{x}_A, -t) * S(t), \quad (10)$$

with \mathbf{x}'_A and \mathbf{x}_A at $\partial \mathbb{D}_A$. $\Gamma^+(\mathbf{x}'_A, \mathbf{x}_A, t)$ and $\Gamma^-(\mathbf{x}'_A, \mathbf{x}_A, t)$ are point-spread functions, which quantify the imperfection of the sampling and the band-limitation, see Figure 5.

Summation representations

We use the point-spread functions introduced in the previous section to transform the integral representations of equations (1) and (2) into summation representations. We start by applying the operation

$$\int_{\partial \mathbb{D}_A} \{\cdot\} * \Gamma^+(\mathbf{x}'_A, \mathbf{x}_A, t) d\mathbf{x}'_A \quad (11)$$

to both sides of equation (1) (with \mathbf{x}_A replaced by \mathbf{x}'_A). Next, by substituting equation (9) in the right-hand side, interchanging the order of summation over $\mathbf{x}^{(i)}$ and integration along $\partial \mathbb{D}_A$,

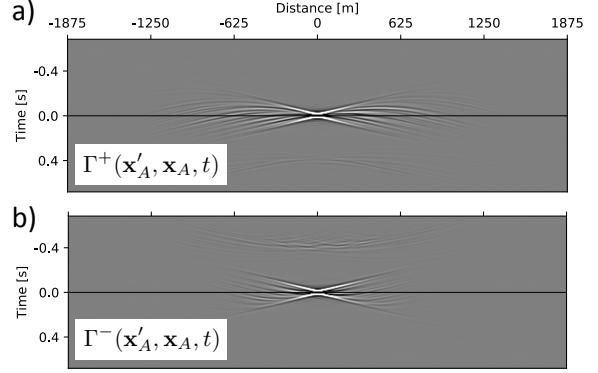


Figure 5: Evaluation of the irregular summations in equations (9) and (10). These point-spread functions quantify the imperfection of the sampling.

substituting equation (6) (with \mathbf{x}_A , \mathbf{x}' and \mathbf{x}'_H replaced by \mathbf{x}'_A , $\mathbf{x}^{(i)}$ and $\mathbf{x}_H^{(i)}$) and using the sifting property of the delta function for the integral along $\partial \mathbb{D}_0$, this gives

$$\hat{G}^{-,+}(\mathbf{x}_R, \mathbf{x}_A, t) + \hat{f}_1^-(\mathbf{x}_R, \mathbf{x}_A, t) = \sum_i R(\mathbf{x}_R, \mathbf{x}^{(i)}, t) * f_1^+(\mathbf{x}^{(i)}, \mathbf{x}_A, t) * S(t), \quad (12)$$

with

$$\hat{G}^{-,+}(\mathbf{x}_R, \mathbf{x}_A, t) = \int_{\partial \mathbb{D}_A} G^{-,+}(\mathbf{x}_R, \mathbf{x}'_A, t) * \Gamma^+(\mathbf{x}'_A, \mathbf{x}_A, t) d\mathbf{x}'_A, \quad (13)$$

$$\hat{f}_1^-(\mathbf{x}_R, \mathbf{x}_A, t) = \int_{\partial \mathbb{D}_A} f_1^-(\mathbf{x}_R, \mathbf{x}'_A, t) * \Gamma^+(\mathbf{x}'_A, \mathbf{x}_A, t) d\mathbf{x}'_A. \quad (14)$$

Note that the right-hand side of equation (12) is identical to the summation in equation (3), which we introduced as the practical implementation of the integral in equation (1). Equation (12) shows that this summation representation leads to a modified Green's function $\hat{G}^{-,+}(\mathbf{x}_R, \mathbf{x}_A, t)$ and a modified focusing function $\hat{f}_1^-(\mathbf{x}_R, \mathbf{x}_A, t)$. These modified functions are specified in equations (13) and (14). According to equation (13), the point-spread function causes a smearing of the source of the Green's function around its source point \mathbf{x}_A . Similarly, equation (14) quantifies the smearing of the focus around the focal point \mathbf{x}_A of the focusing function. We evaluate equations (13) and (14) numerically and add the results together, see Figure 6(a). This figure, which represents the left-hand side of equation (12), is nearly identical to Figure 3(a), which represents the right-hand side of equation (12). Subtraction of these results (not shown) gives a residual, with amplitudes smaller than 0.34% of the maximum of Figure 3(a).

Next, we apply the operation

$$\int_{\partial \mathbb{D}_A} \{\cdot\} * \Gamma^-(\mathbf{x}'_A, \mathbf{x}_A, t) d\mathbf{x}'_A \quad (15)$$

to both sides of equation (2). In a similar way as above we

Marchenko representations for imperfectly sampled data

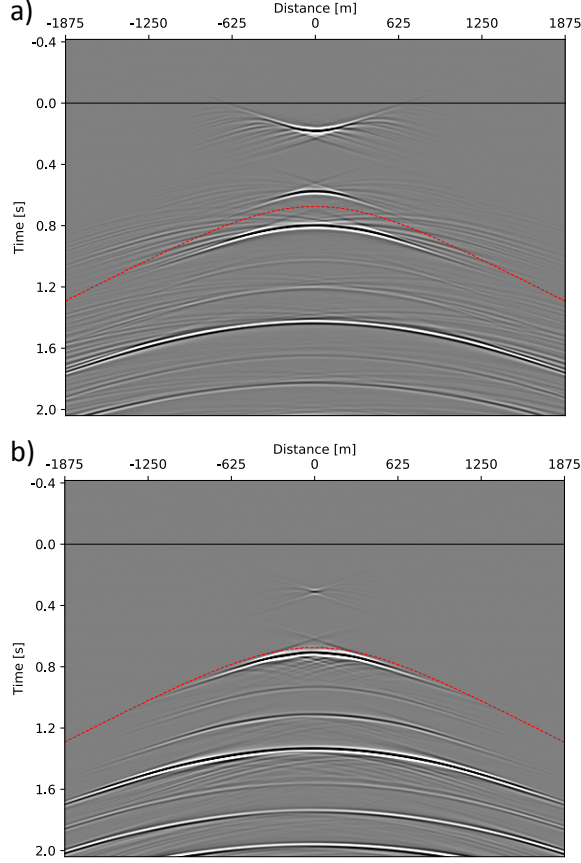


Figure 6: (a) Evaluation of equations (13) and (14) and adding the results together, giving $\hat{G}^{-,+}(\mathbf{x}_R, \mathbf{x}_A, t) + \hat{f}_1^-(\mathbf{x}_R, \mathbf{x}_A, t)$. (b) Evaluation of equations (17) and (18) and adding the results together, giving $\hat{G}^{-,-}(\mathbf{x}_R, \mathbf{x}_A, t) + \hat{f}_1^+(\mathbf{x}_R, \mathbf{x}_A, -t)$.

obtain

$$\hat{G}^{-,-}(\mathbf{x}_R, \mathbf{x}_A, t) + \hat{f}_1^+(\mathbf{x}_R, \mathbf{x}_A, -t) = \sum_i R(\mathbf{x}_R, \mathbf{x}^{(i)}, t) * f_1^-(\mathbf{x}^{(i)}, \mathbf{x}_A, -t) * S(t), \quad (16)$$

with

$$\hat{G}^{-,-}(\mathbf{x}_R, \mathbf{x}_A, t) = \int_{\partial \mathbb{D}_A} G^{-,-}(\mathbf{x}_R, \mathbf{x}'_A, t) * \Gamma^-(\mathbf{x}'_A, \mathbf{x}_A, t) d\mathbf{x}'_A, \quad (17)$$

$$\hat{f}_1^+(\mathbf{x}_R, \mathbf{x}_A, -t) = \int_{\partial \mathbb{D}_A} f_1^+(\mathbf{x}_R, \mathbf{x}'_A, -t) * \Gamma^-(\mathbf{x}'_A, \mathbf{x}_A, t) d\mathbf{x}'_A. \quad (18)$$

The right-hand side of equation (16) is identical to the summation in equation (4). It gives a modified Green's function $\hat{G}^{-,-}(\mathbf{x}_R, \mathbf{x}_A, t)$ and focusing function $\hat{f}_1^+(\mathbf{x}_R, \mathbf{x}_A, -t)$, which are specified in equations (17) and (18). The sum of the numerical evaluation of these equations is shown in Figure 6(b). This figure, which represents the left-hand side of equation (16), is nearly identical to Figure 3(b), which represents the right-hand side of equation (16). Subtraction of these results (not shown)

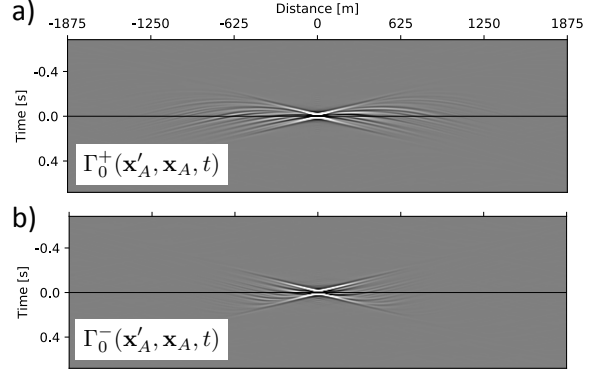


Figure 7: Initial estimates of the point-spread functions, obtained from the direct arrivals of f_1^+ , f_1^- , T and Y .

gives a residual, with amplitudes smaller than 3.31% of the maximum of Figure 3(b).

Towards a modified Marchenko method

The summation representations of equations (12) and (16), with the modified Green's functions and focusing functions defined in equations (13), (14), (17) and (18), form the basis for a modification of the Marchenko method, which accounts for the effects of imperfect sampling. We envisage an iterative scheme, similar to the current Marchenko method, where in each iteration a multi-dimensional deconvolution for the point-spread functions is inserted (between the evaluation of the summation and the application of the time window). This requires an initial estimate of the point-spread functions. To this end we propose to replace the functions f_1^+ , f_1^- , T and Y in equations (9) and (10) by their direct arrivals. For f_1^- and Y further investigation is needed how to define the direct arrivals in general. For the current example this approach leads to reasonable initial estimates of the point-spread functions in Figure 5, see Figure 7.

Conclusions

We have derived summation representations as an alternative for the integral representations which underlie the Marchenko method. These summation representations account for the effects of imperfect sampling. The Green's functions and focusing functions expressed by these representations are distorted by point-spread functions. The summation representations form the basis for a modification of the Marchenko method, which accounts for the effects of imperfect sampling. This modified Marchenko method is subject of ongoing research.

Acknowledgements

We thank Christian Reinicke for his help with the numerical examples. We acknowledge funding from the European Research Council (ERC) under the European Union's Horizon 2020 research and innovation programme (grant agreement No: 742703).

Marchenko representations for imperfectly sampled data

REFERENCES

- Brackenhoff, J., J. Thorbecke, and K. Wapenaar, 2019, Monitoring induced distributed double-couple sources using Marchenko-based virtual receivers: *Solid Earth*, **10**, doi.org/10.5194/se-2018-142.
- Broggini, F., and R. Snieder, 2012, Connection of scattering principles: a visual and mathematical tour: *European Journal of Physics*, **33**, 593–613.
- Pereira, R., D. Mondini, and D. Donno, 2018, Efficient 3D internal multiple attenuation in the Santos Basin: 80th Annual International Meeting, EAGE, Extended Abstracts, We–C–08.
- Ravasi, M., I. Vasconcelos, A. Kritski, A. Curtis, C. A. da Costa Filho, and G. A. Meles, 2016, Target-oriented Marchenko imaging of a North Sea field: *Geophysical Journal International*, **205**, 99–104.
- Staring, M., R. Pereira, H. Douma, J. van der Neut, and K. Wapenaar, 2018, Source-receiver Marchenko redatuming on field data using an adaptive double-focusing method: *Geophysics*, **83**, S579–S590.
- Staring, M., and K. Wapenaar, 2019, Interbed demultiple using Marchenko redatuming on 3D field data of the Santos Basin: 16th International Congress of the Brazilian Geophysical Society, SBGf, Expanded Abstracts, (submitted).
- Van der Neut, J., J. L. Johnson, K. van Wijk, S. Singh, E. Slob, and K. Wapenaar, 2017, A Marchenko equation for acoustic inverse source problems: *Journal of the Acoustical Society of America*, **141**, 4332–4346.
- Van der Neut, J., and K. Wapenaar, 2015, Point-spread functions for interferometric imaging: *Geophysical Prospecting*, **63**, 1033–1049.
- Wapenaar, K., and J. Fokkema, 2006, Green's function representations for seismic interferometry: *Geophysics*, **71**, SI33–SI46.
- Wapenaar, K., J. Thorbecke, J. van der Neut, F. Broggin, E. Slob, and R. Snieder, 2014a, Green's function retrieval from reflection data, in absence of a receiver at the virtual source position: *Journal of the Acoustical Society of America*, **135**, 2847–2861.
- , 2014b, Marchenko imaging: *Geophysics*, **79**, WA39–WA57.
- Wapenaar, K., and J. van der Neut, 2010, A representation for Green's function retrieval by multidimensional deconvolution: *Journal of the Acoustical Society of America*, **128**, EL366–EL371.